# Briefing Space Weather

2023/05/10

This report is for the period from April 24 to 30 (week 1) and May 1 to 8 (week 2).

# 1 Sun

## 1.1 Responsible: José Cecatto

04/24 – No flare; Fast wind stream (=< 500 km/s); 4 CME c.h.c. toward the Earth;
04/25 – No flare; Fast wind stream (=< 600 km/s); 4 CME c.h.c. toward the Earth;
04/26 – No flare; Fast wind stream (=< 550 km/s); 3 CME c.h.c. toward the Earth;
04/27 – No flare; Fast wind stream (=< 450 km/s); 6 CME c.h.c. toward the Earth;
04/28 – M1.8 flare; No fast wind stream; 2 CME c.h.c. toward the Earth *;
04/29 – No flare; Fast wind stream (=< 450 km/s); 12 CME c.h.c. toward the Earth *;
04/30 – M2.4 flare; Fast wind stream (=< 650 km/s); 5 CME c.h.c. toward the Earth;
05/01 – M1.1, M7.1 flares; Fast wind stream (>= 600 km/s) since noon time; 1 CME c.h.c. toward the Earth;
Prev.: Fast wind stream for the next 01-03 days; for the next 2 days (25% M, 01% X) probability of M / X flares; also,
occasionally other CME can present component toward the Earth.
c.h.c. – can have a component; * partial halo; ** halo

Summary

05/01 – M1.1, M7.1 flares; Fast wind stream (=< 500 km/s); 10 CME c.h.c. toward the Earth;
05/02 – No flare; Fast wind stream (=< 550 km/s); 7 CME c.h.c. toward the Earth *,*;
05/03 – M4.2, M3.1, M7.2, M1.7, M2.2 flares; Fast wind stream (=< 500 km/s); 5 CME c.h.c. toward the Earth;
05/04 – M3.9 flare; Fast wind stream (=< 450 km/s); 7 CME c.h.c. toward the Earth *,*;
05/05 – M2.1, M1.2 flares; Fast wind stream (=< 500 km/s); 9 CME c.h.c. toward the Earth *;
05/06 – No flare; Fast wind stream (=< 550 km/s); 11 CME c.h.c. toward the Earth;
05/07 – M1.5, M1.6 flares; Fast wind stream (=< 500 km/s); 2 CME c.h.c. toward the Earth *;
05/08 – No flare; Fast wind stream (=< 550 km/s); 2 CME c.h.c. toward the Earth;
Prev.: Fast wind stream for the next 01-02 days; for the next 2 days (55% M, 15% X) probability of M / X flares; also,
occasionally other CME can present component toward the Earth.
c.h.c. – can have a component; * partial halo; ** halo

# 2 Interplanetary medium

## 2.1 Responsible: Paulo Ricardo Jauer

- The modulus of the interplanetary magnetic field component showed a maximum peak of 31 nT on Apr/24 at 01:30 UT during the analyzed period.
- Two peaks of 16 nT and 17 nT were also detected on April 6 and 7 at 04:30 and 15:30 UT respectively.

- The BxBy components presented variations in the analyzed period, keeping both oscillating within the interval [+15, -30] nT, without the presence of sector change. The IMF By component showed a minimum value of -30 nT on Apr/24 at 10:30 UT.

- The component of the bz field showed a minimum value on 24/Apr at 02:30 UT of -29 nT. During the interaction of the CME-type structure that interacted with the global and inner magnetosphere. The Bz component also showed a minimum value on May 06 at 03:30 UT of -13 nT.

- The solar wind density showed peaks on 23/Apr 06/May and 07/May at 19:30, 03:30 and 14:50 UT of 27, 30 and 29 $p/cm^3$ due to interplanetary structure interaction.

- The solar wind speed remained on average above 400 km/s with a peak on 28/Apr at 16:30 UT of 691 km/s.

- The position of the magnetopause was oscillating with a minimum value recorded on 23/Apr at 19:30 UT of 5.9 Re and on 06/May at 03:30 UT of 6.8 Re. On average, the position of the magnetopause was above the equilibrium position.

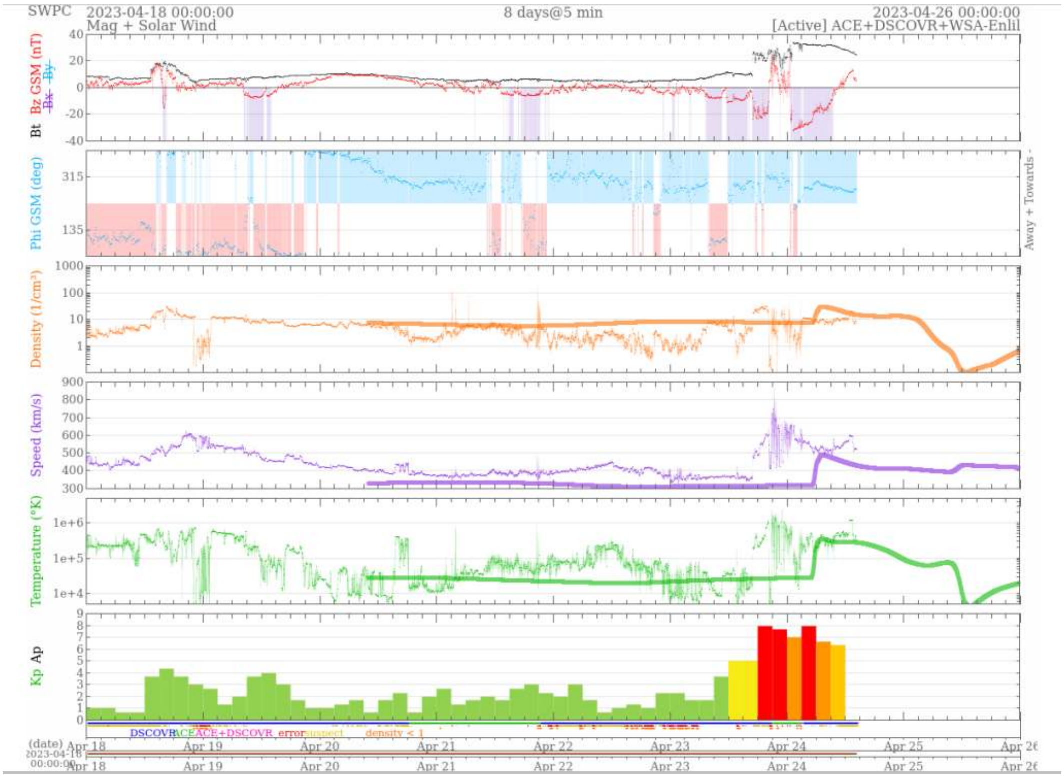


Figura 1: Week 1.

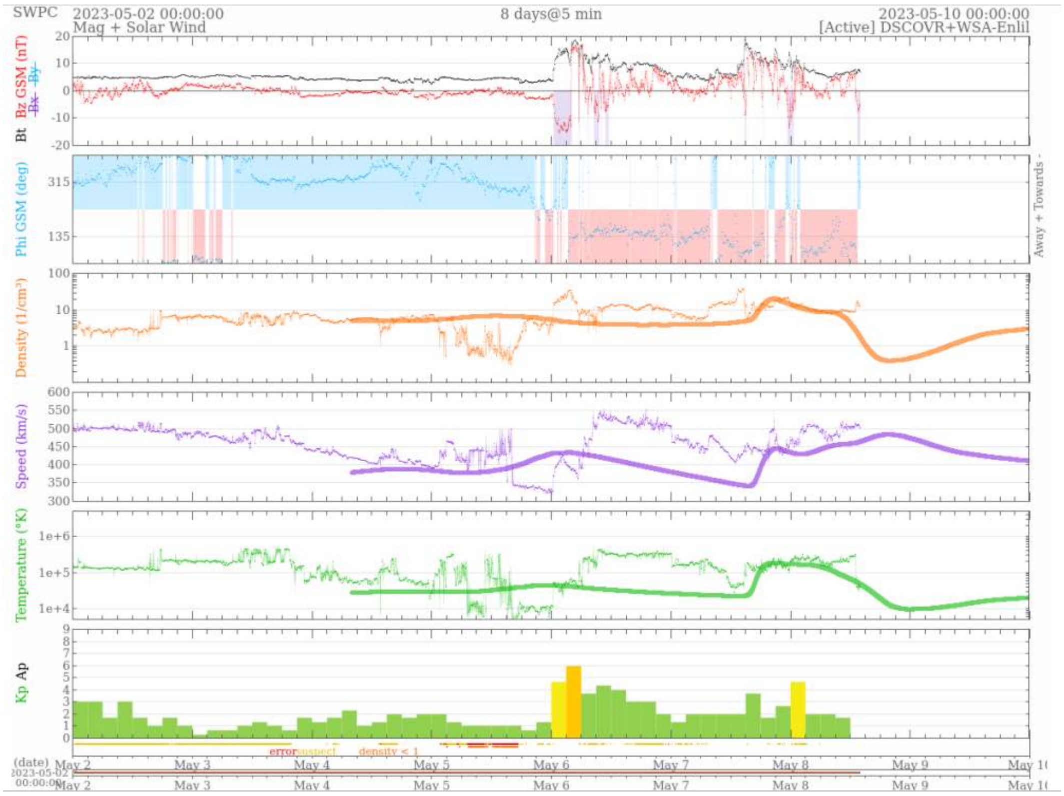


Figura 2: Week 2.

# 3 Radiation Belts

## 3.1 Responsible: Ligia Alves da Silva

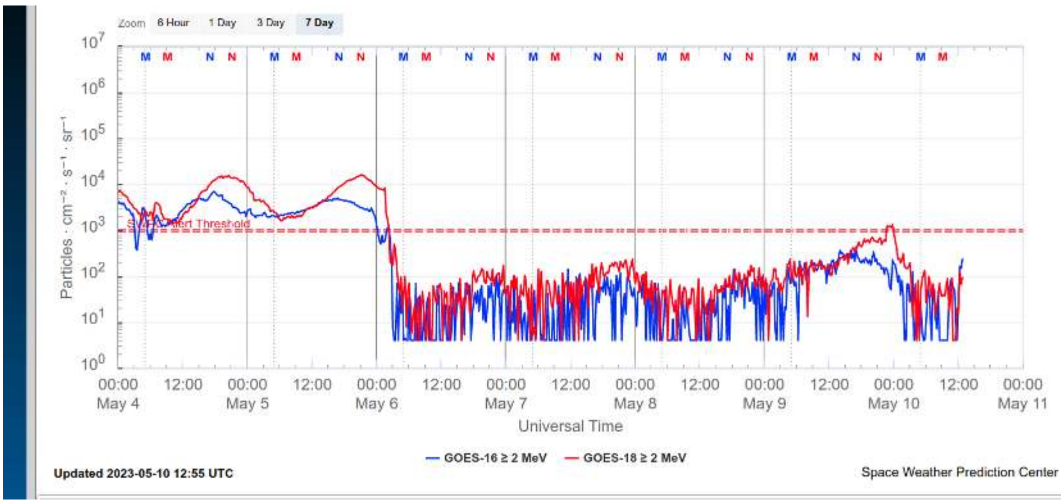


Figura 3: High-energy electron flux (> 2 MeV) obtained from GOES-16 and GOES-18 satellite. Source: `https://www.swpc.noaa.gov/products/goes-electron-flux`

High-energy electron flux (> 2 MeV) in the outer boundary of the outer radiation belt obtained from geostationary satellite data GOES-16 and GOES-18 (Figure 3) shows a strong dropout of approximately three orders of magnitude at the beginning on the 6th of May. This decrease in electron flux persists for almost three days, showing a significant increase at 00:00 UT on 10/May which reached $10^3$ particles/($cm^2 ssr$).

# 4 ULF waves

## 4.1 Responsible: Graziela B. D. Silva

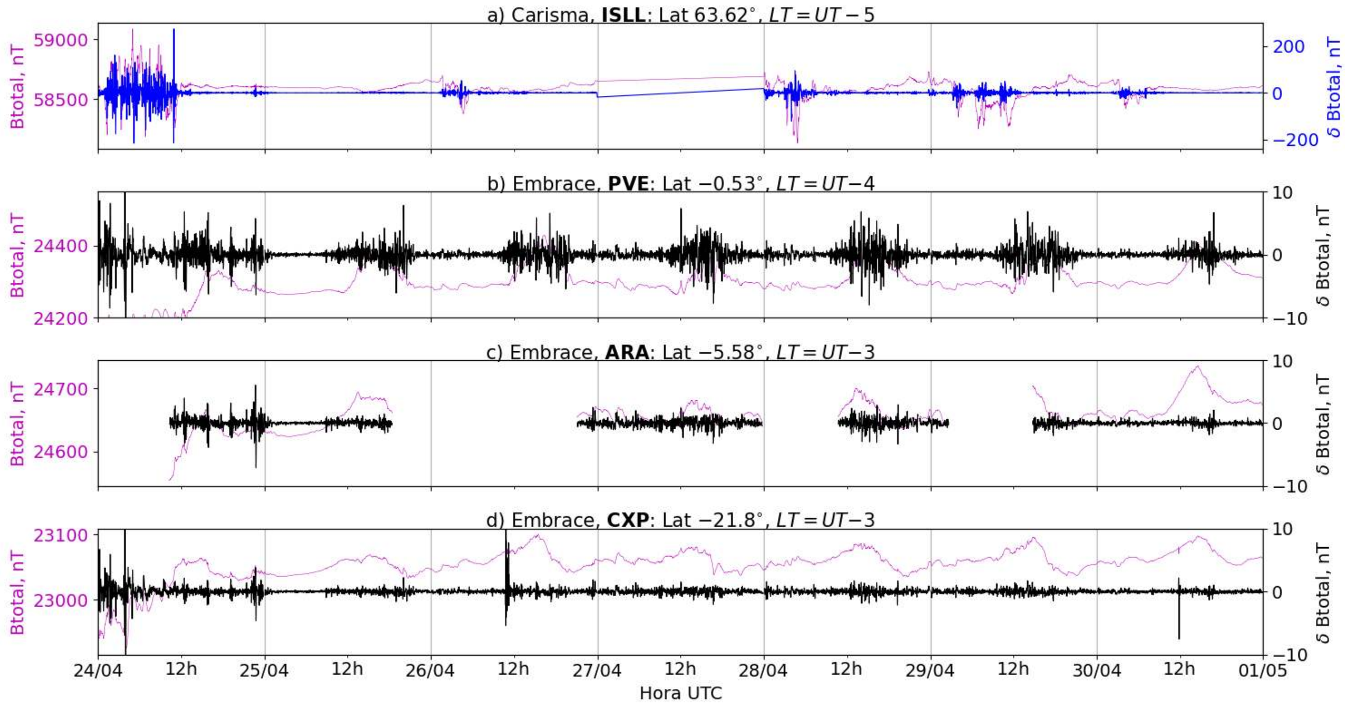


Figura 4: Week 1: a) Timeseries of the geomagnetic field total component measured at ISLL station (Island Lake) of the CARISMA magnetometer network in magenta, along with the associated perturbation in the Pc5 band shown in blue. b-d) timeseries of the geomagnetic field total component measured at stations PVE (Porto Velho), ARA (Araguatins), and CXP (Cachoeira Paulista) of the EMBRACE network in magenta, along with the Pc5 perturbation in blue.

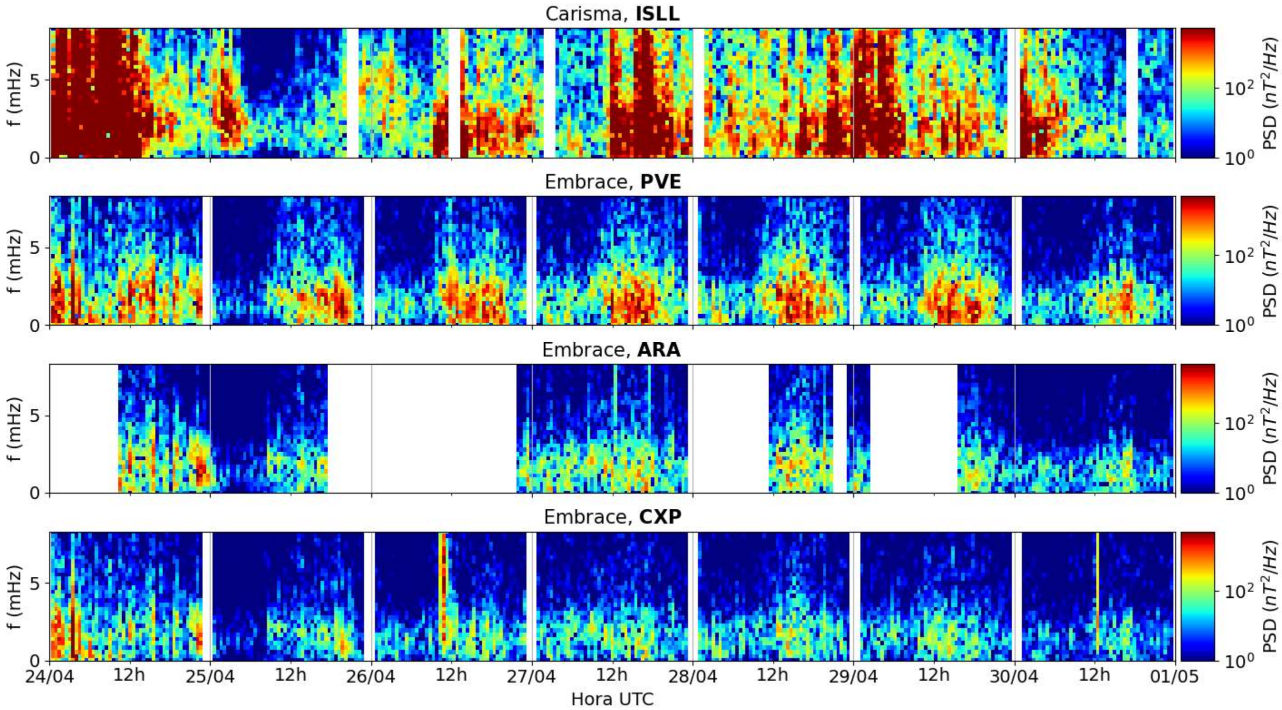


Figura 5: Week 1: a-d) Time evolution of the power spectral density obtained from the filtered timeseries of the geomagnetic field total component ($\delta$ Btotal) for a) the high latitude station (ISLL-CARISMA), and b-d) for the low latitude stations of EMBRACE (PVE, ARA, CXP).

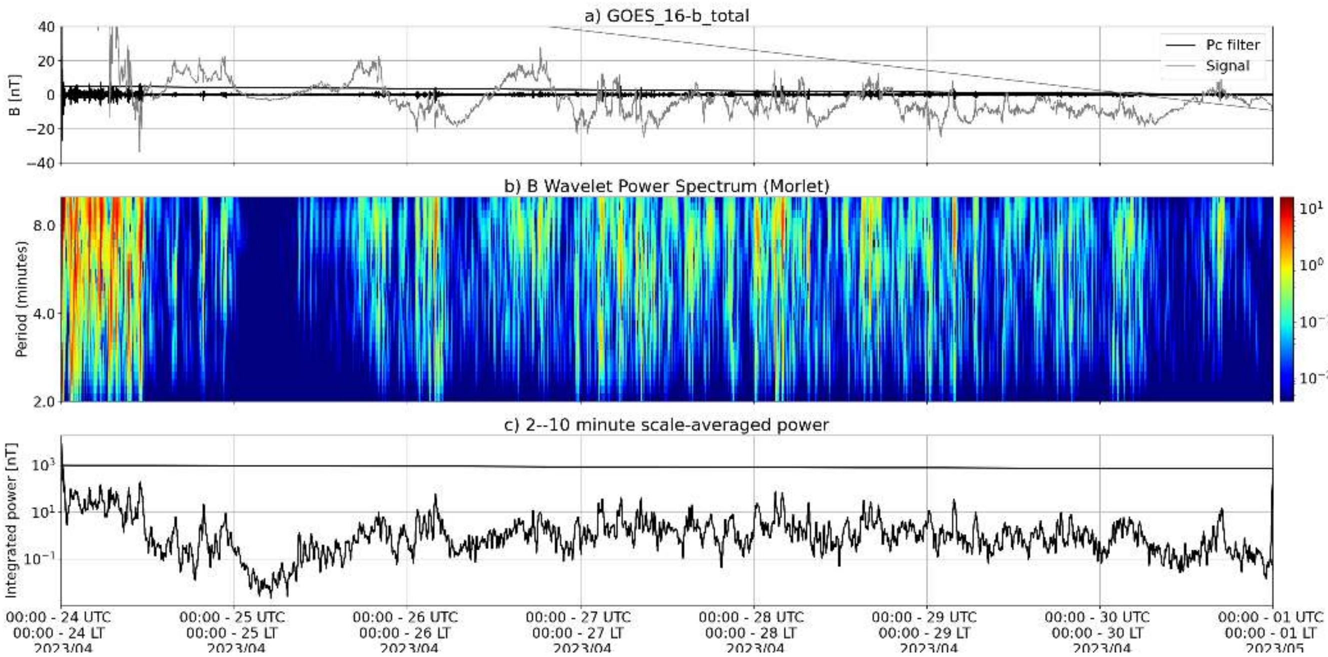


Figura 6: Week 1: a) Timeseries of the geomagnetic field total component measured by GOES 16, together with the Pc5 fluctuation in black. b) Wavelet power spectrum of the filtered timeseries. c) Average ULF power in the period range from 2 to 10 minutes.

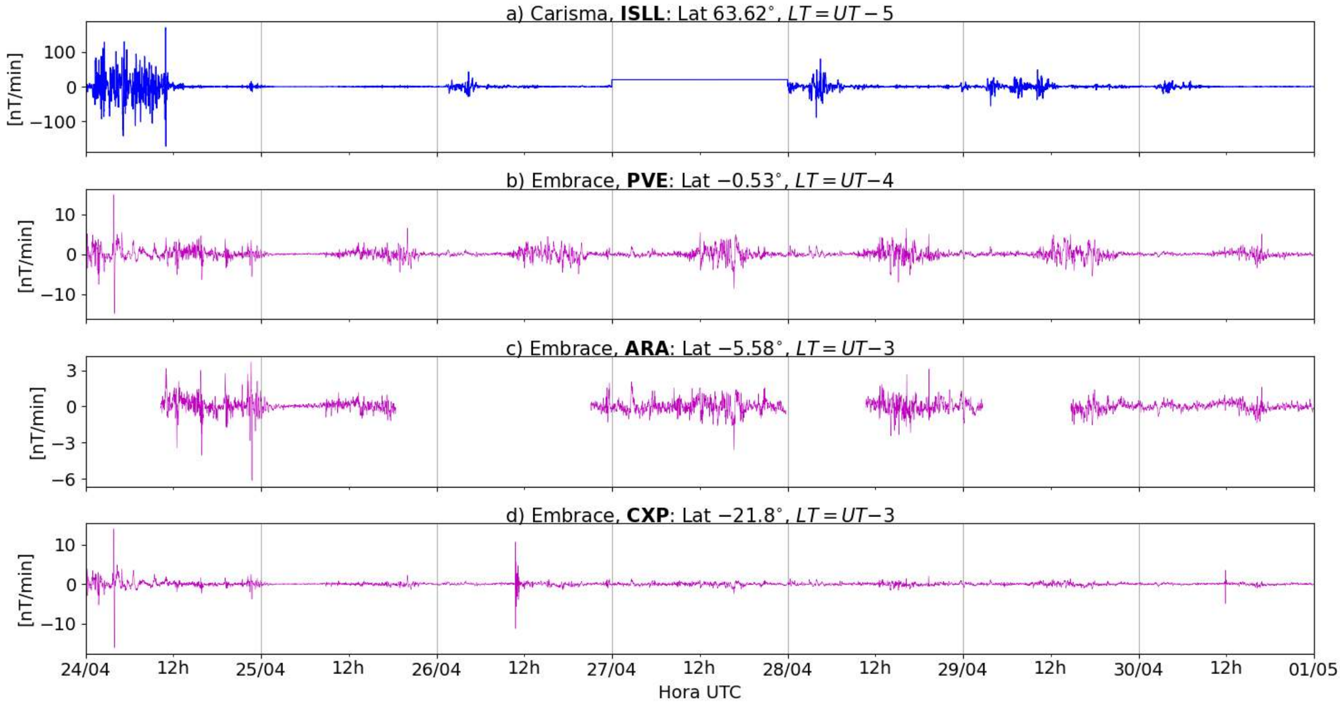


Figura 7: Week 1: a-d) The rate of change of the geomagnetic field total component (dB/dt) obtained for a) the high latitude station (ISLL-CARISMA), and b-d) for the low latitude stations of EMBRACE (PVE, ARA, CXP).

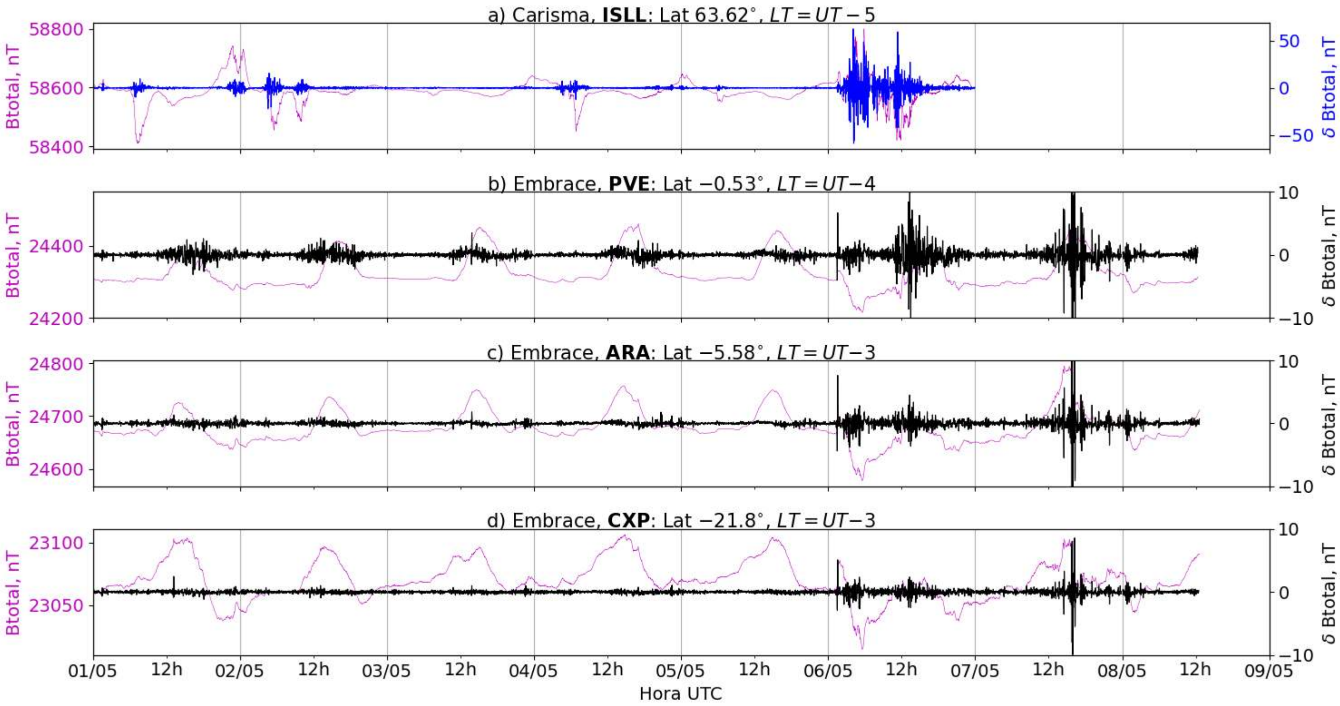


Figura 8: Week 2: a) Timeseries of the geomagnetic field total component measured at ISLL station (Island Lake) of the CARISMA magnetometer network in magenta, along with the associated perturbation in the Pc5 band shown in blue. b-d) timeseries of the geomagnetic field total component measured at stations PVE (Porto Velho), ARA (Araguatins), and CXP (Cachoeira Paulista) of the EMBRACE network in magenta, along with the Pc5 perturbation in blue.

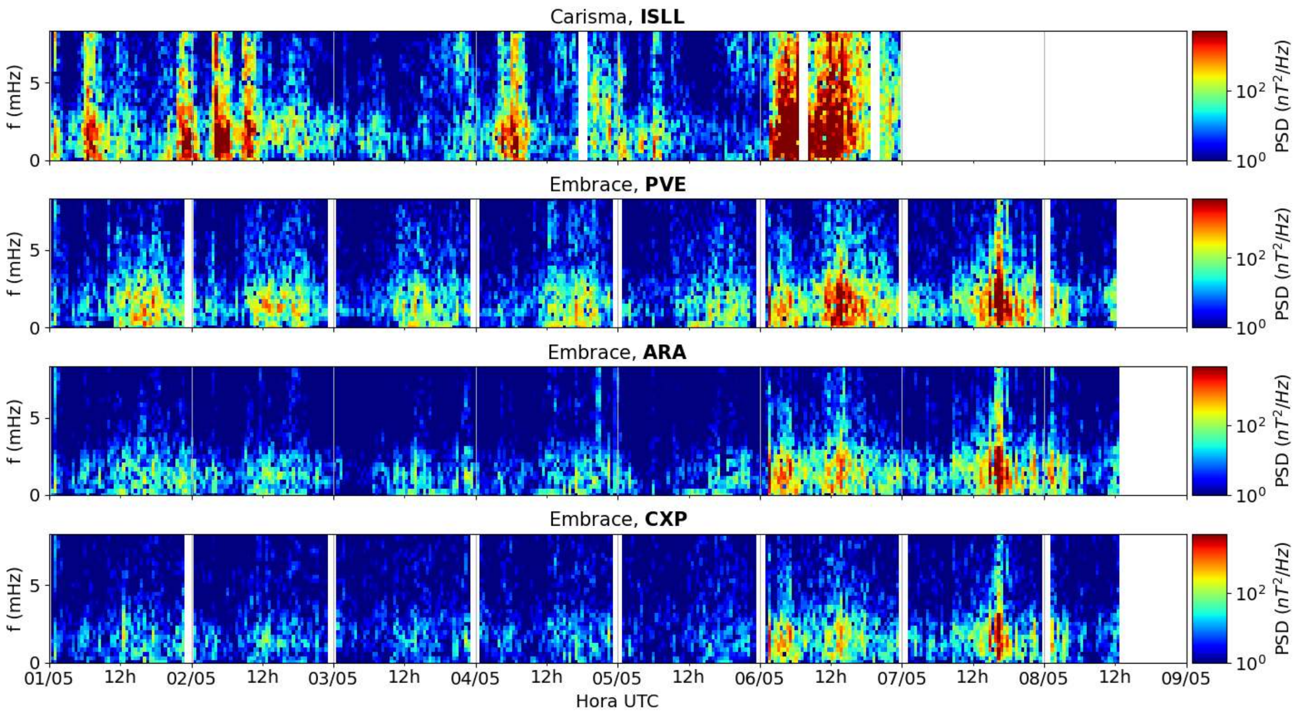


Figura 9: Week 2: a-d) Time evolution of the power spectral density obtained from the filtered timeseries of the geomagnetic field total component ($\delta$ Btotal) for a) the high latitude station (ISLL-CARISMA), and b-d) for the low latitude stations of EMBRACE (PVE, ARA, CXP).

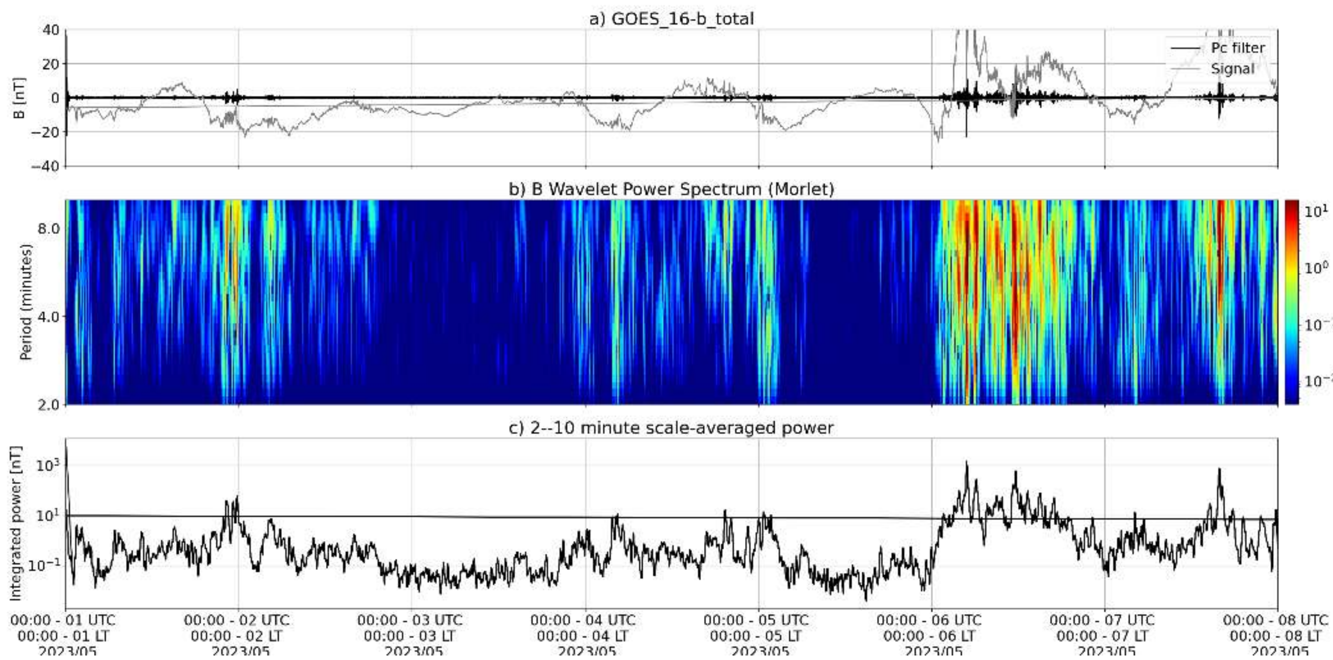


Figura 10: Week 2: a) Timeseries of the geomagnetic field total component measured by GOES 16, together with the Pc5 fluctuation in black. b) Wavelet power spectrum of the filtered timeseries. c) Average ULF power in the period range from 2 to 10 minutes.

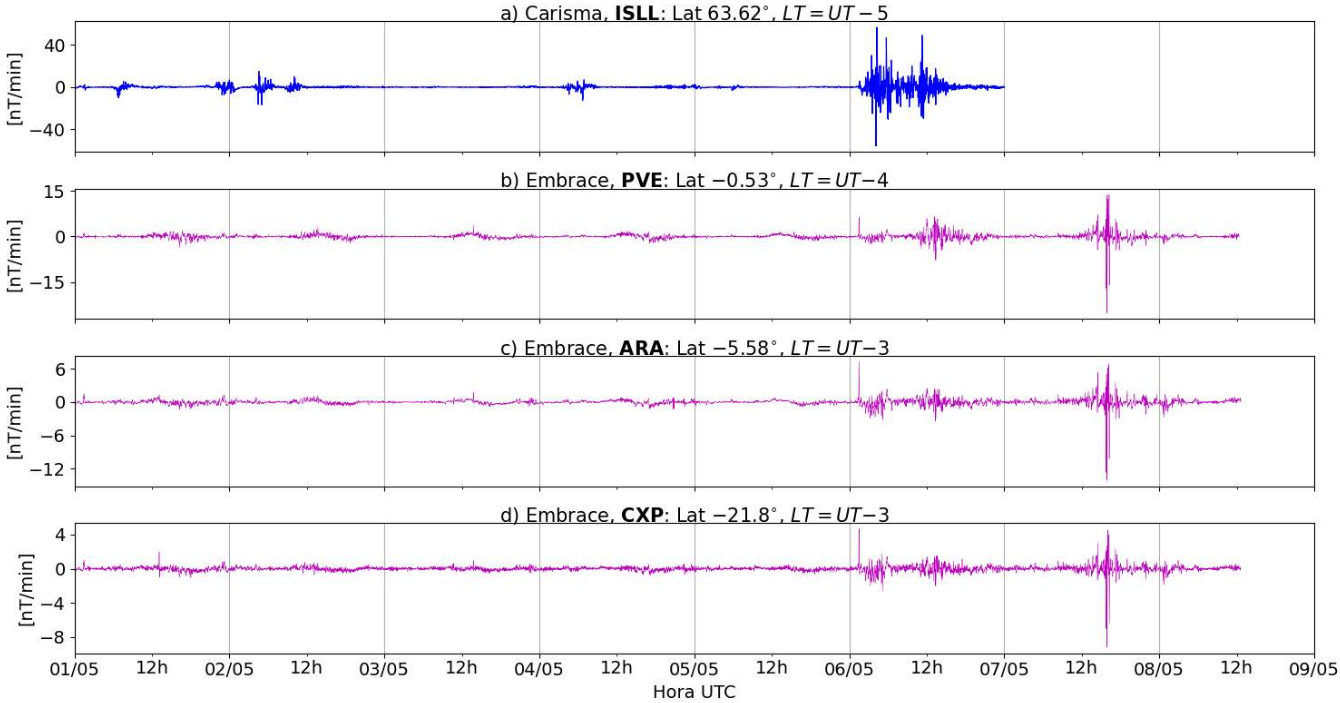


Figura 11: Week 2: a-d) The rate of change of the geomagnetic field total component (dB/dt) obtained for a) the high latitude station (ISLL-CARISMA), and b-d) for the low latitude stations of EMBRACE (PVE, ARA, CXP).

- The GOES 16 satellite in geosynchronous orbit (L $\sim$ 6.6) registered significant activity of Pc5 ULF waves over the week 1, especially on April 24, and as of May 6 during week 2.
- As observed on the ground, the ISLL station at high latitude registered significant levels of ULF wave activity on this day and over the week 1. In week 2, there was an intense activity registered only on May 6.
- The PVE station from Embrace MagNet, located under the dip equator, registered significant levels of recurrent ULF wave activity over the week 1. In week 2, such activity was considered low until May 5. Later, it highly increased.
- The CXP and ARA stations at low latitudes of Brazil rather registered low activity of the waves over the whole week 1, but April 24. In week 2, as noted for PVE, the wave activity was low until the 5th, and then increased as of May 6.
- The dB/dt rates were enhanced on April 24 up to values ¿ 100 nT/min in ISLL (high latitude) and about or below 12 nT/min in magnitude at the low latitudes of Brazil. There was occurrence of sudden impulses on April 24. In week 2, the magnitude of dB/dt rates reached 40 nT/min in ISLL and $\sim$ 15 nT/min on May 6 and 7, respectively.

# 5 Geomagnetic activity

## 5.1 Responsible: Lívia Alves

The following figures show the geomagnetic indices during week 1 and week 2, both reported. It is observed that the intense geomagnetic storm of 4/23 had a Dst minimum of -212 nT reached at 7 UT of 4/24. The auroral activity on 04/23 was intense, with the AE index exceeding 2000 nT after 20 UT. In week 2, it is observed that the moderate geomagnetic storm of 06/05 had a Dst minimum of -75 nT reached at 6 UT, and the AE index was above 1500 nT shortly after 3 UT.

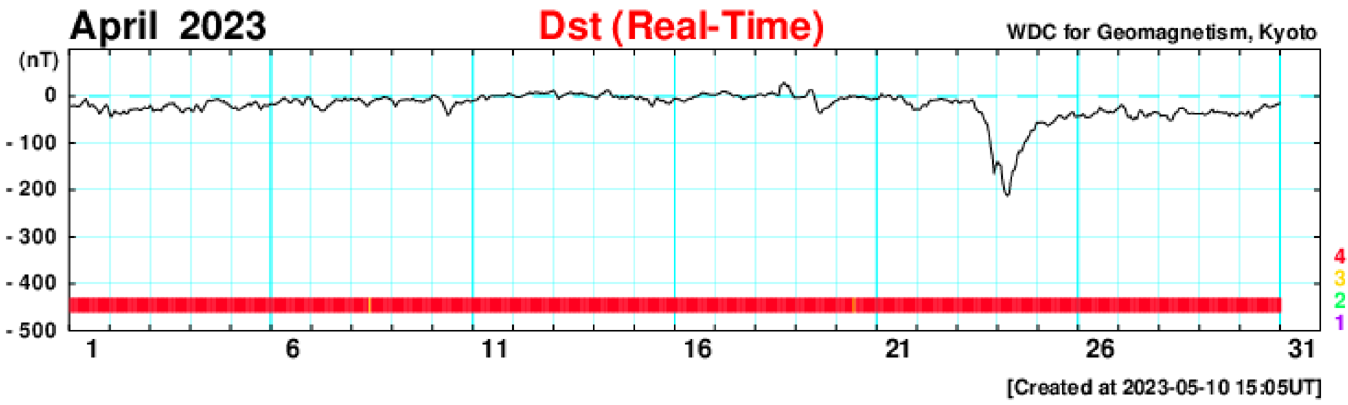


Figura 12: Time evolution of the Dst index during week 1.

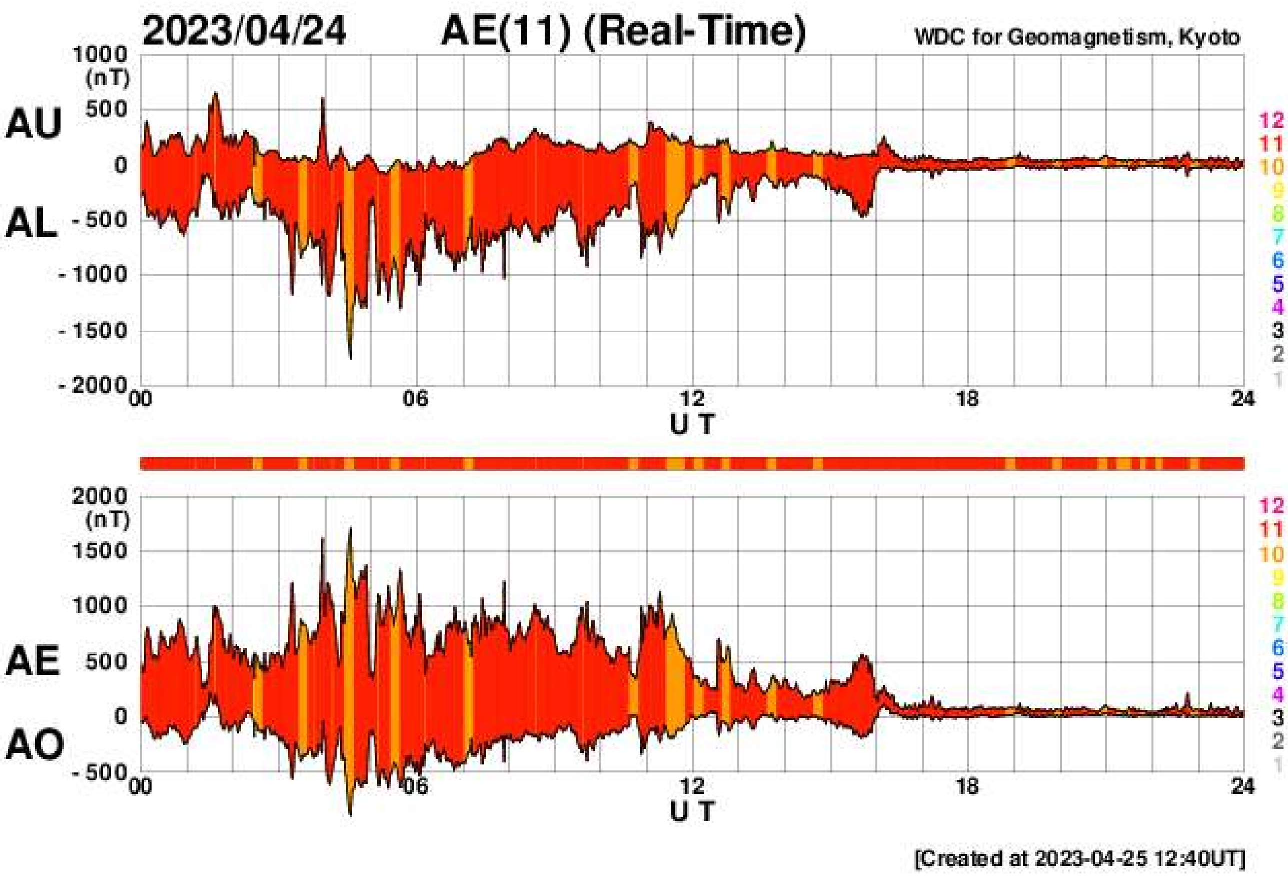


Figura 13: Time evolution of the AE index through 04/24.

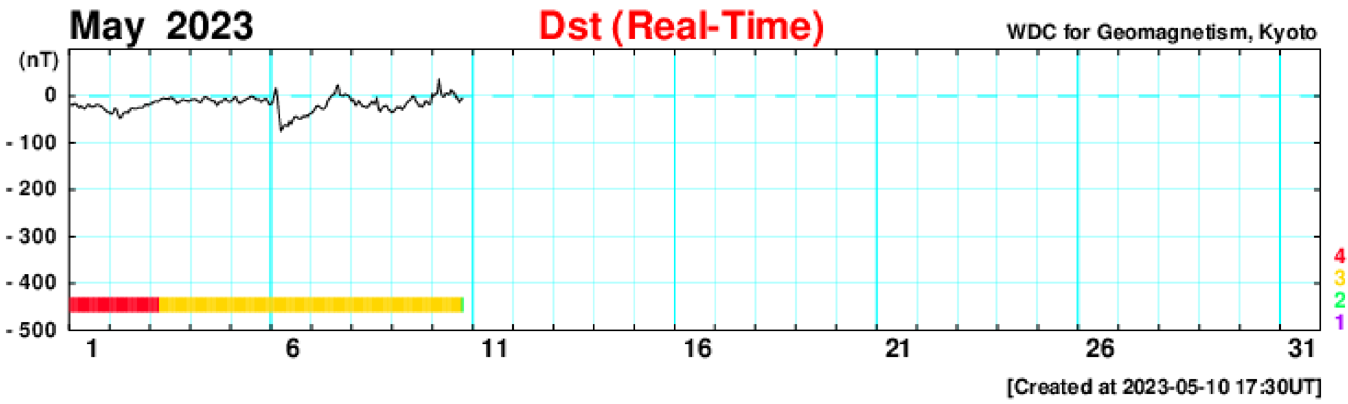


Figura 14: Time evolution of the Dst index during week 2.

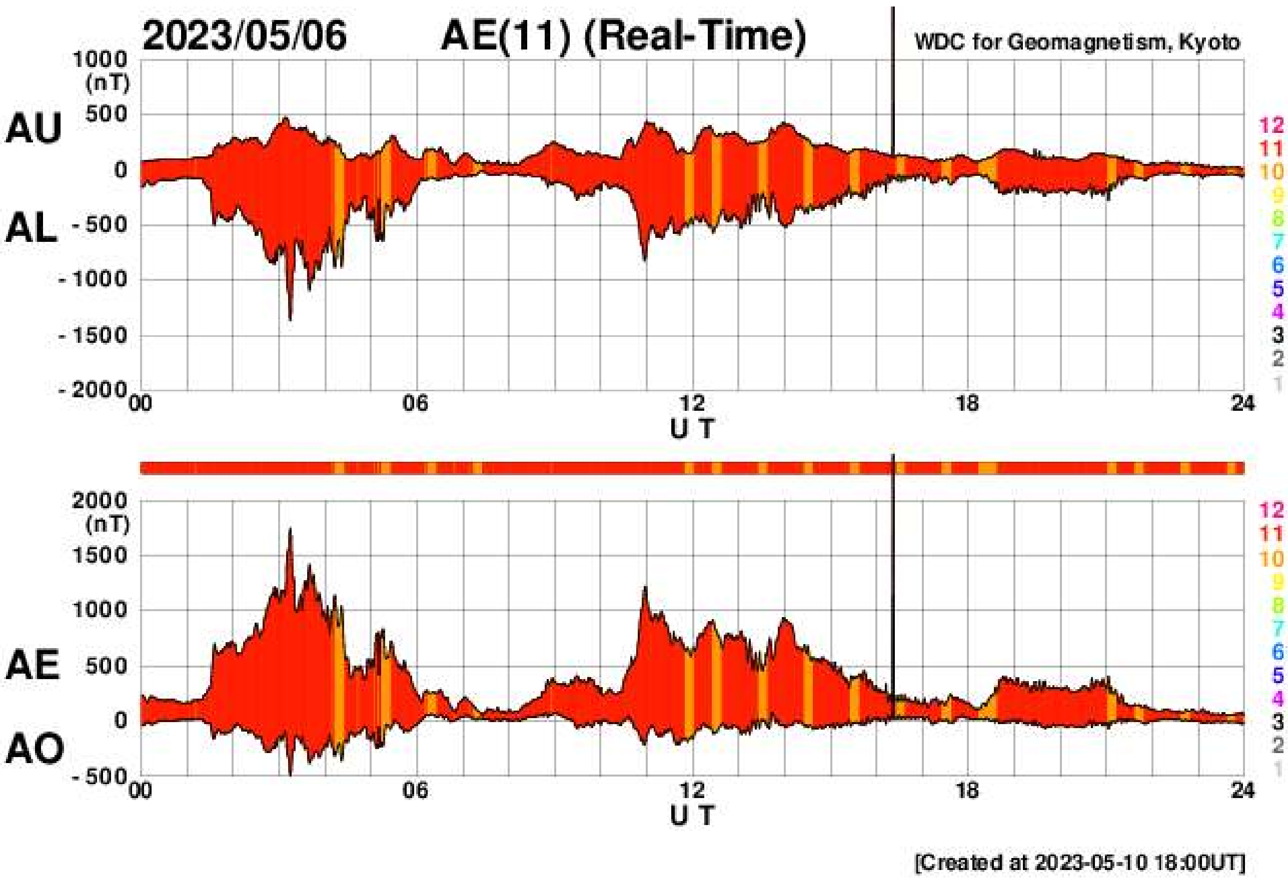


Figura 15: Time evolution of the AE index through 05/06.

# 6 Ionosphere

## 6.1 Responsible: Laysa Resende

**Cachoeira Paulista:**

- There were not spread F during all days in this week.
- The Es layers reached scale 5 on Apr, 27.

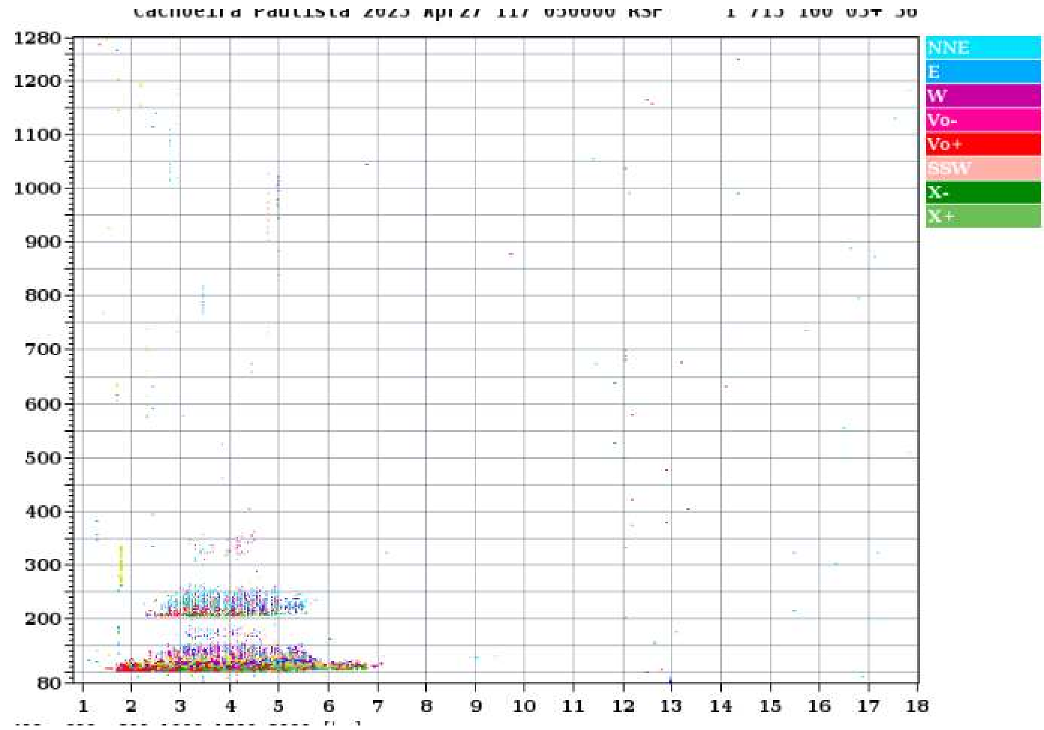


**Fortaleza**

- There were spread F on April 30.
- The Es layers reached scale 5 between 24 and 26.

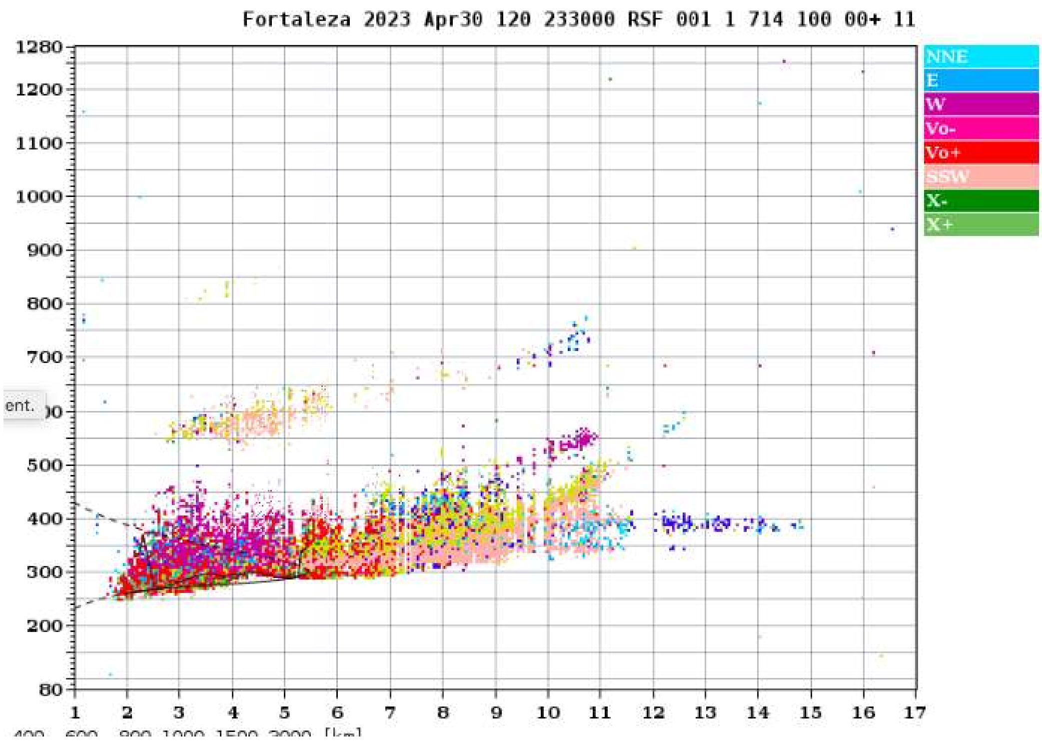

# 7 ROTI

## 7.1 Responsible: Carolina de Sousa do Carmo

In the week 2259 (April 23 to 29, 2023) there were no ionospheric irregularities (plasma bubble), on all analyzed days. Figure 1 shows the ROTI time series for four stations in the Brazilian sector (Natal (RNNA), Bacabal (MABB), Cuiabá (CUIB) and São José dos Campos (SJSP)).

In the week 2260 (April 30 to May 6, 2023) there were no ionospheric irregularities (plasma bubble), on all analyzed days. Figure 1 shows the ROTI time series for four stations in the Brazilian sector (Natal (RNNA), Bacabal (MABB), Cuiabá (CUIB) and São José dos Campos (SJSP)).

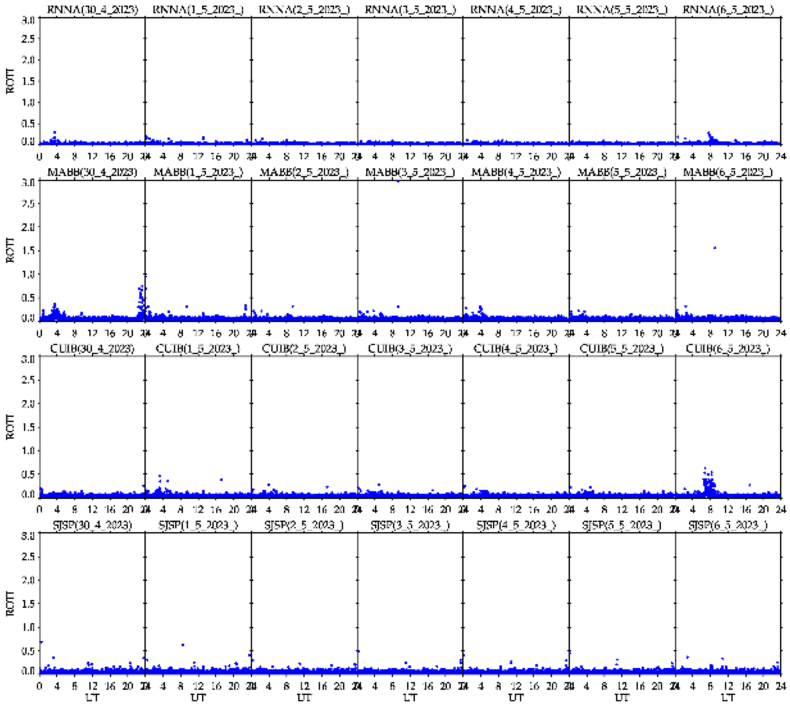


Figura 16: ROTI time series for four stations in the Brazilian sector (Natal (RNNA), Bacabal (MABB), Cuiabá (CUIB) and São José dos Campos (SJSP)), from April 23 to 29, 2023.

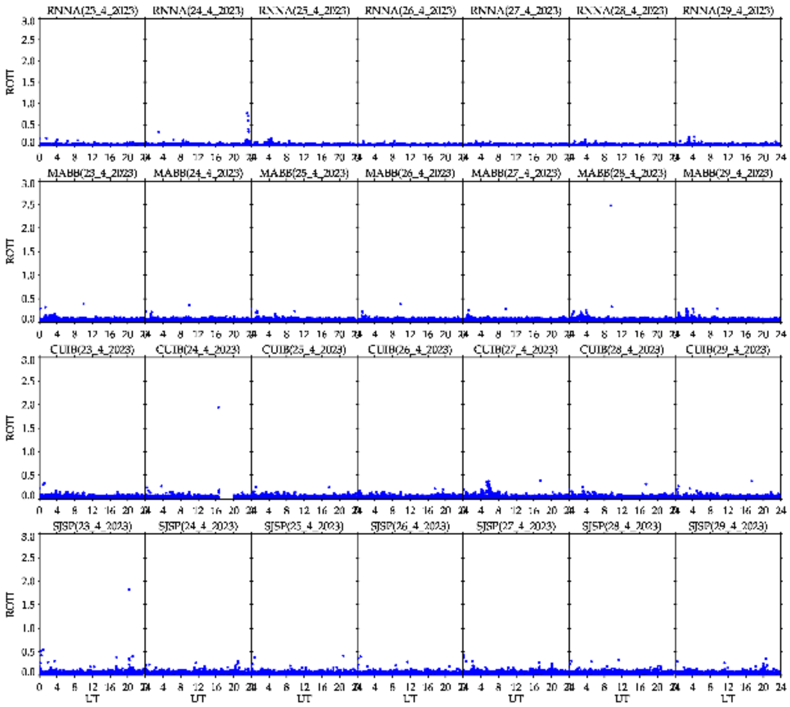


Figura 17: ROTI time series for four stations in the Brazilian sector (Natal (RNNA), Bacabal (MABB), Cuiabá (CUIB) and São José dos Campos (SJSP)), from April 30 to May 6, 2023.